

Electrospun silk fibroin/fibrin vascular scaffold with superior mechanical properties and biocompatibility for its applications as tissue engineering

Lei Yang¹, Xu Wang², Xiong Man³, Xinfang Liu¹, Sidong Luo¹, jinxian Luo¹, and yang Wang¹

¹Guangdong Second Provincial General Hospital

²Guangdong University of Technology

³Guangzhou University of Chinese Medicine

July 19, 2023

Abstract

Electrospun scaffolds have been highly important in the fields of regenerative medicine and vascular tissue engineering. Developing a vascular scaffold with structural and functional natural vascular-mimicking scaffold is our key task. The mechanical properties of artificial vascular as a key issue for successful transplantation in small diameter tissue engineering blood vessels. Herein, we blended silk fibroin (SF) and fibrin to fabricate the composite scaffold by electrospinning to overcome the insufficiency of mechanical properties of fibrin. Subsequently, morphological characteristics, mechanical properties, hydrophilicity, hemocompatibility, degradation and cytocompatibility of SF/fibrin (0:100), SF/fibrin (15:85), SF/fibrin (25:75) and SF/fibrin (35:65) scaffolds were carefully investigated, respectively. According to these results in vitro, SF/fibrin (25:75) vascular scaffold was implanted subcutaneously, and then it's in vivo degradation and histocompatibility were analyzed. The fiber structure of SF/fibrin hybrid scaffold exhibited smooth and uniform, and the fiber diameter of this scaffolds were relatively small. Compared with fibrin scaffold, the mechanical strength of SF/fibrin scaffold increased obviously, but the hydrophilicity was correspondingly weakened gradually. Meanwhile, the results showed that all SF/fibrin scaffolds indicated excellent blood compatibility and appropriate biodegradation rate. SF/fibrin (25:75) scaffold could improve the proliferation and adhesion of MSCs. The results of animal experiments confirmed that the degradation of SF/fibrin (25:75) scaffold was faster than that of SF scaffold, and it could effectively promote tissue regeneration and cell infiltration. All in all, SF/fibrin (25:75) electrospun scaffold had balanced and controllable biomechanical, degradability, and good cell compatibility. Thus, the scaffold was an ideal candidate material for artificial blood vessels.

Electrospun silk fibroin/fibrin vascular scaffold with superior mechanical properties and biocompatibility for its applications as tissue engineering

Lei Yang¹, Xu Wang⁵, man Xiong⁶, Xinfang Liu², Sidong, Luo^{2,4}, Jinxian Luo⁷, Yeyang Wang^{2,3,4*}

1. Department of Surgical base, Guangdong Second Provincial General Hospital, Guangzhou, China
2. Department of Spine, Orthopaedic Center, Guangdong Second Provincial General Hospital, Guangzhou, China
3. Zhaoqing Central People's Hospital, Zhaoqing, Guangdong, China
4. The Second School of clinical medicine, Southern Medical University, Guangzhou, China
5. Biomedical college, Guangdong University of Technology, Guangzhou, China

6. School of Nursing, Guangzhou University of Chinese Medicine, Guangzhou, China

7. Thyroid and mammary surgery department, Guangdong Second Provincial General Hospital, Guangzhou, China

* Corresponding authors. E-mail addresses: wyysmu@163.com (Yeyang Wang).

Abstract

Electrospun scaffolds have been highly important in the fields of regenerative medicine and vascular tissue engineering. Developing a vascular scaffold with structural and functional natural vascular-mimicking scaffold is our key task. The mechanical properties of artificial vascular as a key issue for successful transplantation in small diameter tissue engineering blood vessels. Herein, we blended silk fibroin (SF) and fibrin to fabricate the composite scaffold by electrospinning to overcome the insufficiency of mechanical properties of fibrin. Subsequently, morphological characteristics, mechanical properties, hydrophilicity, hemocompatibility, degradation and cytocompatibility of SF/fibrin (0:100), SF/fibrin (15:85), SF/fibrin (25:75) and SF/fibrin (35:65) scaffolds were carefully investigated, respectively. According to these results in vitro, SF/fibrin (25:75) vascular scaffold was implanted subcutaneously, and then it's in vivo degradation and histocompatibility were analyzed. The fiber structure of SF/fibrin hybrid scaffold exhibited smooth and uniform, and the fiber diameter of this scaffolds were relatively small. Compared with fibrin scaffold, the mechanical strength of SF/fibrin scaffold increased obviously, but the hydrophilicity was correspondingly weakened gradually. Meanwhile, the results showed that all SF/fibrin scaffolds indicated excellent blood compatibility and appropriate biodegradation rate. SF/fibrin (25:75) scaffold could improve the proliferation and adhesion of MSCs. The results of animal experiments confirmed that the degradation of SF/fibrin (25:75) scaffold was faster than that of SF scaffold, and it could effectively promote tissue regeneration and cell infiltration. All in all, SF/fibrin (25:75) electrospun scaffold had balanced and controllable biomechanical, degradability, and good cell compatibility. Thus, the scaffold was an ideal candidate material for artificial blood vessels.

Keywords :SF/fibrin scaffold; mechanical strength; electrospun; vascular; tissue engineering

Introduction

According to the survey and research of WHO, cardiovascular diseases (CVDs), as a disease with a mortality rate much higher than other diseases, seriously endangers the health of people all over the world¹. By 2019, the disease has caused more than 18 million deaths and 390 million disabilities. According to reports from relevant departments, the number of deaths caused by CVDs may be 23.4 million by 2030.² Worse still, CVDs impose an enormous economic burden on many countries.³⁻⁴ Moreover, the probability of congenital cardiovascular diseases (CCDs) is approximately 0.7% among newborns. Each year, the number of new cases of CCDs reaches up to 200,000 in China.⁵ Nowadays, revascularization has been common believed as a satisfactory treatment for severe CVDs and CCDs by most of medical workers, aimed to relieve myocardial ischemia or reduce myocardial damage. Specifically, whether to adopt intervention therapy or coronary artery bypass surgery depends on the severity of them. autologous vessels with good biocompatibility such as greater saphenous vein, has been considered as the most preferred source of blood vessels by researchers. Unfortunately, they are always under-resourced, anatomical variations, etc.⁶ Regarding this, we should develop suitable artificial vascular scaffolds to address needs for the treatment this disease.

Even though many studies have confirmed that synthetic vascular grafts of large diameter vessels ($\varnothing > 6$ mm) have been successfully used in clinical practice for more than 70 years.⁷ Regrettably, it is hard to obtain ideal results once the material has been applied to small diameter vessels ($\varnothing < 6$ mm). This is attributed to its relatively low patency rate, susceptibility to calcification, thrombosis and neointimal hyperplasia.⁸ What is worse, these drawbacks have seriously hindered the further development of the vascular graft. Nevertheless, it is notable that tissue engineering as a valuable approach, has the potential to overcome the problems of currently these grafts. Herein, we should develop a small diameter vascular scaffold close to autologous vessels with mechanical and biological characteristics, which can work stably under hemodynamic conditions, which will spark a profound medical revolution to the treatment of the disease.

Currently, a large number of synthetic polymer materials mainly including Silk fibroin, polycaprolactone, polyurethane and poly(L-lactide-co- ϵ -caprolactone) i.e, have been widely used in the research of small diameter tissue engineered vascular grafts.⁹⁻¹⁰ On the one hand, there are some advantages like superior biocompatibility, mechanical properties and cell affinity. On the other hand, there are some disadvantages like insufficiency in degradability and biological stability, typically hydrophobic, which are unfavorable to cell proliferation and adhesion. Consequently, many investigators always focus on the combination polymers. To compensate for their shortcomings, researchers usually blended native materials and polymer materials to successfully prepare an ideal composite material. For example, Ikram et al.¹¹ used fibrin as adjuvant to fabricate mechanically stable SF/fibrin biocomposites by using simple and scalable technology, and finally confirmed that the composite materials can be used in cardiovascular tissue engineering.

SF is a natural polymer, usually derived from mulberry *Bombyx mori* cocoons. Furthermore, many scientists have confirmed that SF is an ideal biological scaffold material due to its excellent mechanical properties, low immune reaction, superior biocompatibility, various polymer modification sites and bioactive sites.¹² Whereas, its application in vascular tissue engineering is hindered by its insufficient processability and slow degradation. Compared with other natural biomaterials, Fibrin has the following advantages and become a research hotspot in recent years. It can be obtained from the patient's own blood, and its preparation is relatively inexpensive and completely autologous. In addition, it has an admirable bioactive matrix, thereby promoting biochemical molecules and cell delivery systems.¹³ Unfortunately, fibrin has also some disadvantages like insufficiency in rapid degradation and insufficient mechanical properties, many scientists generally incorporate it into composite vascular materials for application.¹⁴

In the present study, four different types of SF/fibrin vascular scaffolds by electrospinning were developed and designed. The composite scaffolds could be greatly improved their mechanical properties and biocompatibility. The morphology, structure, hydrophilicity, biomechanical properties, hemocompatibility and degradation in vitro of as-fabricated different SF/fibrin vascular materials with electrospinning technology was comprehensively investigated. Furthermore, the biological properties of the prepared different scaffolds were evaluated by cytocompatibility test and in vivo implantation characterization. Based on the above test, we hypothesized that the electrospinning of SF/fibrin vascular scaffold with an optimum mass ratio can withstand certain mechanical strength similar to native blood vessels. Eventually, their potentialities as hybrid scaffolds for small diameter tissue engineering.

Materials and methods

2.1 Materials

Fibrin was provided by Thermo Fisher (Wuhan, China). *Bombyx mori* silk cocoons were obtained from Chuangseed Biomaterials Company (Guangzhou, China). 98% formic acid and Dulbecco's Modified Eagle Medium (DMEM) was obtained from Dingguo Biotechnology Co., Ltd (Zhengzhou, China). Cell Counting kit-8, Masson staining kit, CD68, hematoxylin eosin staining kit and Live Cell Staining Kit were acquired from APEX BIO Technology LLC (Shanghai, China). Fetal bovine serum, actin antibody, DAPI, Triton-X100, PBS and 4% polyformaldehyde solutions were purchased from Weigo Technology Co., Ltd (Guangzhou, China).

2.2 Fabrication of SF/fibrin vascular materials

For some work similar to prepare SF/fibrin vascular scaffolds by electrospinning, our research team has abundant experience and achieved satisfactory scientific research results.¹⁵⁻¹⁶ The first thing was that we had to implement SF extraction. *Bombyx mori* silk cocoons were prepared into smaller pieces and soaked in ethanol for 48 hours. Next, we put them in Na₂CO₃ aqueous (0.5% w/v) solution and boiled them for an hour with the material to liquor ratio of 1:100. This operation was carried out at a temperature of 100. Subsequently, the as-degummed silk fibroin was washed with distilled water multiple times, and then dried in the oven for 24 hours. Then, they dissolved in CaCl₂-CH₃CH₂OH-H₂O (mole ratio =1: 2: 8) at 76±2 for 5min. After that, SF solution was dialyzed against distilled water for about 72h. SF solutions were lyophilized before they were stored.¹⁷⁻¹⁸ Briefly, SF/fibrin with mass ratios of 0:100, 15:85, 25:75 and

35:65 were dissolved into formic acid solvent to obtain a fixed mixing concentration (10% wt), respectively. They were placed on a shaking table and shaken for 12 hours to prepare some homogeneous electrospinning solutions. The parameter values of the electrospinning instrument (ET, Ucalery, China) were established as: curing distance (12 cm), volume flow rate (0.8 mL/h) and spinning voltage (18 kV). Different SF/fibrin nanofibers were obtained after the polymer solution was cured by high voltage electricity. Eventually, the prepared scaffold was dried and ventilated to eliminate the residual solvent.

2.3 Exploration of SF/fibrin scaffolds under SEM

Scanning electron microscopy (SEM, Hitachi SU8100, Japan) was used to analyze the morphological changes of SF/fibrin vascular scaffolds. All samples were prepared with the same area size, sputtered with gold for half a minute, and then observed under SEM with an acceleration voltage of 10kV. We used the method to evaluate the mean fiber diameter distribution of electrospun materials by Image J software. Fifty nanofibers were randomly chosen, and their mean diameters were analyzed, and then the corresponding images were drawn.

2.4 Contact angle examination

The hydrophobicity of different SF/fibrin vascular scaffolds was measured by contact angle equipment (Fangrui, China). In order to this end, four different samples were prepared into a square of 1 cmx1 cm and placed them on the stage. Afterwards, we placed the different samples on the stage and sequentially dropped syringes with distilled water onto the surface of the sample. These images were collected using a camera after 5 seconds of the droplet deposited. The contact angle was calculated by computer software. In the meantime, these experimental samples were checked three times and the mean value was achieved (n=3).

2.5 Investigation of mechanical test in vitro

2.5.1 Burst strength

To obtain the ideal burst strength value, four different tested samples were completely hydrated in PBS for 20 minutes (n=3). Then, we fixed the sample on the equipment by 3-0 silk sutures and the other end was blocked. We steadily injected PBS solution into the samples until the vascular scaffolds ruptured. We used the CPT2500 USB installation to record the maximum pressure data before the failure of the test samples and took it as the burst strength value.

2.5.2 Suture strength

The suture strength of the vascular scaffolds meets the standards of the China Association of Medical Devices Industry (CAMDI), which fully guarantees its safety and effectiveness. We prepared different vascular materials with a length of about 2.0 cm, and fixed them at one end of the instrument with 6-0 polypropylene sutures. The other end was located in the grip, and the looseness of the equipment before their operation was checked. Next, we operated with an invariable elongation rate until failure of the samples and the maximum load of the samples prior to tearing off was retained. These values were considered as the size of suture strength (n=3).

2.5.3 Tensile properties

The mechanical properties of four different SF/fibrin scaffolds in axial directions were examined by using a universal material testing machine (WDW-10, Yanrun, China). The as-prepared materials were sequentially split into 2.0 cmx1.0 cm sizes, and the electrospun materials of each sample were evaluated. To assessment the tensile strength of the materials, we adjusted the appropriate parameter values tested in the device. The mechanical properties of different samples were measured by testing equipment. Each test samples were checked three times, and the mean value was analyzed and obtained.

2.6 Assessment of blood-materials compatibility

2.6.1 Hemolysis assay

The biological safety of the vascular scaffolds with the blood cells was evaluated by hemolysis experiment. Fresh anticoagulated blood from SD rats was thoroughly mixed with normal saline, and then 2% of the mixture was prepared. Diluted blood solution (0.2mL) was placed in the sterilized SF/fibrin samples respectively. The mixture was placed in a container at 37 and incubated for half an hour. Then, different sample solutions were centrifuged for 10 minutes at 1500 r/min. The supernatant was retained in a 96-well plate, and examined by the absorbance value of the microplate analyzer (Microplate, China) at 540 nm. These samples were tested three times to get the mean value. The components of the positive group were diluted blood (0.2mL) and distilled water (3.8mL). However, diluted blood (0.2mL) and normal saline (3.8mL) were combined with the negative group. The analysis formula of hemolysis rate (HR) was as follows:

$$HR (\%) = \frac{Dt - D_{nc}}{D_{pc} - D_{nc}} \times 100\%$$

Here, Dt indicated the absorbance of the test scaffold, Dnc referred to the absorbance of negative control, and Dpc showed the absorbance of the positive control.

2.6.2 Platelet adhesion test

To obtain fresh anticoagulant whole blood, we mixed fresh blood from SD rats and sodium citrate. Moreover, we placed it in an instrument and centrifugation at 1000 rpm for 15 mins to get the supernatant, which was platelet-rich plasma (PRP). Then, different samples of nanomaterials were sterilized by ultraviolet radiation for about 2 hours, and they were safely placed in 24-well plates. In addition, we repeatedly used PBS for rinsing to obtain clean electrospun materials. The prepared PRP was soaked in different vascular materials and incubated in 37 degC water baths for 1 hour. The PBS was washed, and then 2.5% glutaraldehyde was immobilized, and the gradient of alcohol was dehydrated. After the test samples were dried, we observed the platelet adhesion morphology of the samples by a SEM and collected some images, respectively.

2.6.3 Co-incubation of red blood cells and materials assay

Referring to the previous operation, we centrifuged the whole blood, and then removed the supernatant to get compressed red blood cells. After that, we added an appropriate amount of PBS buffer to wash it twice. The different sterilized vascular scaffolds were evenly placed on a 24-well plate, and red blood cell solution (700μL) was successfully added to each well. We used a pipette to repeatedly blow and aspirate to mix them evenly with the sample. They were incubated for 3 hours in a water bath at 37 . After drying the sample satisfactorily, the microscopic morphology of red blood cells on the vascular scaffold was analyzed under SEM and photos were collected.

2.6.4 Plasma recalcification time experiment

To analyze the time of blood coagulation with the vascular materials in calcium-free anticoagulant plasma after calcium ion was added again. Platelet-poor plasma (PPP) was established by centrifuging fresh whole blood at 1800 r/min for 30 min. Four different samples were made 4 cm×4 cm and kept in each sterile tube. Then, 200μL PPP and 200μL CaCl₂ solutions were added to each tube, respectively. Hereon, it was explained that TCP as the control group without any vascular scaffold material. We observed the earliest time of fibrin formation and recorded its data. Each group of samples was evaluated three times, and the mean value was achieved.

2.6.5 Coagulation function trial

To study the anticoagulant properties of the vascular material, we used APTT and TT method to evaluate them. In this operation, the sterilized vascular scaffolds were made into a disc shape and stored in a tube. Then, plasma (1 m) from rats was added and incubated for 1 hour. The time was analyzed by a coagulation equipment (SYSMEX CA-7000, Japan). It should be noted here that the non-vascular substance group was used as the control group. Note that these experimentally obtained data had to be checked three times consecutively.

2.7 Evaluation of biodegradation of electrospun materials in vitro

To operate the in vitro degradation experiment of different SF/fibrin composite scaffolds, as-obtained samples were made into 1 cm×1 cm size. Subsequently, the tested samples were immersed in PBS (pH 7.4) and lipase solution (pH 7.4, 1 mg/mL) successively, and incubated at 37. After incubation at different specific time points respectively, the weight of different samples were obtained, and then the mass loss rate was carefully evaluated by the degradation calculation method (n=3). The formula of degradation mass loss was frequently used in our previous work.¹⁵ For which I would like to emphasize that the PBS solution should be added once a week and the lipase solution was supplemented once a week.

2.8 Study on cell-materials compatibility

2.8.1 Cell grown behavior with materials extracted

To investigate the compatibility of material extract and cells together, the Rabbit adipose-derived mesenchymal stem cells (RADMSCs, Guangdong Medical Laboratory Animal Center, China) with different scaffold materials were co-cultured. We put them on the culture plate and cultured them at a density of 1×10^4 /mL. Subsequently, the cells were stored in an incubator (37,5% CO²) and incubated for 2, 4 and 6 days, respectively. Here, the cells without materials were the control group. We regularly update the culture medium every 2 days. Thereafter, the cells were analyzed by a microscope and these images were obtained.

2.8.2 Cell proliferation on scaffold material

An CCK-8 kit was widely used to quantitatively analyze the proliferation of the cell after different predetermined time points of culture, respectively. To begin with, four different scaffold materials were prepared into appropriately sized circular discs and RADMSCs were co-incubated, and then retained in 96-well plates at 1, 3, and 7 days. After that, we subsequently added DMEM and CCK-8 overnight under dark light, and rinsed repeatedly three times with sterile PBS. Meanwhile, they were incubated in an incubator (37) for 4 hours. Ultimately, the absorbance value in different specific time periods was evaluated at the wavelength of 540 nm by using full-automatic multifunctional enzyme analyzer equipment (Berthold, Germany).

2.8.3 Live cell staining test

After the prepared samples were satisfactorily sterilized by ultraviolet rays, and they were laid on a 48 well plate. Then, DMEM and 1×10^4 cells were added to per well orderly, and incubated subconfluency in a CO₂ incubator at 37. It was worth noting that the specific medium should be updated every 2 days. Furthermore, Calcein-AM solution with an ideal ratio was prepared in accordance with the requirements of living cell staining kit instructions. The waste liquid was sucked and the cells with PBS were rinsed to remove impurities. In the dark, we evenly added the prepared staining solution to each well plate (100μL). They were wrapped in tin foil and incubated at 37 for 30 minutes. We repeatedly rinsed it with PBS. Different samples were observed under an inverted fluorescence microscope (DMIL, China) and some pictures were collected at different times.

2.8.4 Immunofluorescence trial

All the different SF/fibrin electrospun vascular scaffolds were made into 1.0 cm×1.0 cm sizes. The test samples were sterilized for 2 hours. We washed them repeatedly with PBS and soaked them. Besides, 20μL of 1×10^4 RADMSCs were co-incubated with different sample materials at the specific time point. After 4 and 7 days of culturing, we washed it with PBS for 3 times and fixed it with 4% polyoxymethylene solution. Simultaneously, we used 0.2% Triton-X100 to permeate it for 10 minutes, and obstructed it with 1% bovine serum albumin at 4. Actin antibodies were added to each well at the dark and placed in an incubator for 1h at 37, and then stained with DAPI for half an hour in a dark room temperature. Afterwards, we used a fluorescence microscope (DMIL, China) to observe all the tested samples and collected these images. We evaluated the number of cells on each different sample from random fields of view (FOV) by Image J software. Each test sample was evaluated three times.

2.9 Exploration of the related properties of electrospun scaffold in vivo

2.9.1 Animal experiments

The subcutaneous implantation assay *in vivo* was followed in accordance with the Animal Care and Experiment Committee guidelines. The experimental protocol was approved by the Animal Ethics Committee of Guangdong Second Provincial General Hospital (Guangdong, China). The Sprague Dawley rats (7 weeks male, average weight:100g) were selected from Guangdong Second Provincial General Hospital.12 rats were arbitrary grouped into 3 groups and electrospun scaffolds were implanted *in vivo*: Control group (n=4), SF vascular scaffolds (n=4) and SF/fibrin (25:75) vascular scaffolds (n=4). The prepared samples of the appropriate size were irradiated by ultraviolet light, soaked in ethanol and rinsed with PBS, respectively. In short, SD rats were anesthetized by inhalation of isoflurane and firmly fixed them on the operating table. Then, we removed the hair in the operation region with an electric razor and sterilized it with 75% medical alcohol. After that, a surgical incision about 2 cm long was cut on the dorsal area of the rat, and the subcutaneous pockets were gently separated with vascular forceps. Note that during the operation, we had to protect the important nerves and blood vessels of rats. We implanted the different sterilized samples into the pockets, and then closed the subcutaneous tissue separately. Moreover, we should pay attention to the principle of aseptic operation. All the as-operated rats continued to drink water and eat food regularly. After implantation operation at a specific time point, these rats were sacrificed safely, and electrospun scaffolds with surrounding tissues were removed for analysis and investigation.

2.9.2 Weightlessness of electrospun scaffold

To investigate the degradability of different vascular scaffolds *in vivo*, we sacrificed SD rats at specific time points. These materials implanted *in vivo* were extraction, and air-dried to remove excess water. In addition, the weight of electrospun scaffolds were evaluated by electronic balance. The formula for calculating the weight loss rate was as follows.

$$\text{Weight loss rate (\%)} = \frac{W_1 - W_2}{W_1} \times 100\%$$

W_1 showed the dehydrated of the vascular scaffold before implantation, and W_2 showed the dehydrated of the test sample after implantation.

2.9.3 Tissue staining analysis

The SD rats were sacrificed by overdose of anesthetics after 1 and 2 weeks, respectively. Here, it was need to be emphasized that one rat died unexpectedly during the implementation of this animal experiment. The cause of death was unknown, and the survival rate was 91%. Then, the implanted scaffolds with the surrounding tissues were successfully collected. We used 4% polyformaldehyde solutions for fixation and ethanol with different concentrations for dehydration, and embedded with fixed paraffin. Different test samples were prepared into cross-sectional slices (thickness 5 μ m) by microtome (SM2500, Leica, Nussloch, Germany). We stained these slices by hematoxylin-eosin (H&E), Masson's trichrome staining and CD68, respectively. Eventually, all images were observed and collected by an inverted fluorescence microscope (DMIL, China).

2.10 Statistical analysis

This data was indicated by the mean \pm standard deviation(SD). Each group in the experiments should be calculated at least 3 times. We used GraphPad Prism 7 and OriginPro2018 software for statistical analysis. The one-way AVOVA method was applied to compare the mean values among each group. The value of $p < 0.05$ showed a significant difference.

3. Results

3.1 Preparation and morphology of SF/fibrin vascular scaffolds

SF and fibrin were considered as raw materials, and a series of SF/fibrin vascular scaffolds with different mass ratios were designed and developed by an electrospinning system(Fig.1A).The results showed that four different SF/fibrin electrospun films had been successfully fabricated with the size of 1.2 cm (length) \times 1.2 cm (width) (Fig.1B1-B4). To further explore the internal microscopic morphology of the vascular scaffolds, we found under the SEM that the nanofiber structure of four different SF/fibrin scaffolds were smooth,

without obvious bead-like defects, and the fibers were randomly distributed (Fig.1C1-C4). What's more, we randomly chose 50 nanofibers under the SEM and evaluated their fiber diameters by ImageJ software. The analysis showed that the mean fiber diameters of SF/fibrin(0:100), SF/fibrin(15:85), SF/fibrin(25:75) and SF/fibrin(35:65) were $732\pm 33\text{nm}$, $513\pm 15\text{nm}$, $424\pm 11\text{nm}$ and $397\pm 12\text{nm}$, respectively (Fig.1D1-D4).

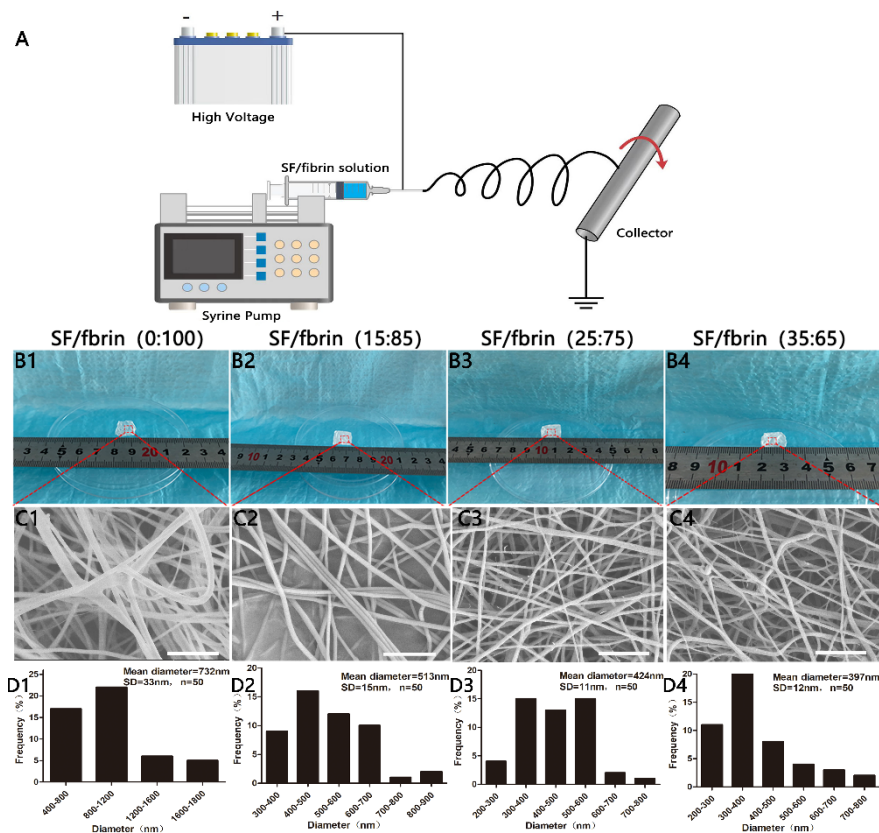


Fig. 1. Fabrication and characterization of the electrospun vascular scaffold. Schematic diagram of electrospun SF/fibrin hybrid scaffolds(A). The macroscopic appearance of SF/fibrin scaffolds with different mass ratios(B1-B4). SEM images of four electrospun scaffolds(C1-C4). Scale bars:10 μm . Fiber diameter distribution of different SF/fibrin scaffolds by ImageJ software (D1-D4) (n=3).

3.2 Hydrophilicity and mechanical characterization of SF/fibrin scaffolds

To analyze its hydrophilic properties, the water contact angle of the samples was evaluated. The results from water contact angle experiment showed that the contact angle of SF/fibrin (0:100) electrospun scaffold was about 22.1°. Furthermore, we also observed that the contact angle data of the four scaffolds increased with the increase of SF content, and the water contact angle of SF/fibrin (35:65) vascular scaffold was 34.6°, which confirmed that the increased of SF/fibrin mass ratio had affected their contact angle value (Figure 2A).

In the tissue engineering vascular scaffold, the key measurement index is burst pressure. When the SF content in the SF/fibrin composite scaffolds added from 15% to 35%, the burst pressure increased from $1729\pm 48\text{mmHg}$ to $2267\pm 97\text{mmHg}$, respectively. Moreover, the results showed that the burst pressure of SF/fibrin (0:100), SF/fibrin (15:85), SF/fibrin (25:75) and SF/fibrin (35:75) scaffolds were significant differences (Figure 2B).

Suture strength of vascular scaffold as an important evaluation index will affect the success or failure of

artificial vascular scaffold transplantation. The suture strength data of four SF/fibrin electrospun scaffolds increased significantly with the increased of SF. Interestingly, suture strength of SF/fibrin (15:85), SF/fibrin (25:75) and SF/fibrin (35:65) scaffolds were analogous to that of native arteries. Meanwhile, the suture strength values of four SF/fibrin scaffolds were statistically significant (Figure 2C).

The ideal electrospun scaffold material should have excellent mechanical strength, which can maintain the stability of its structure and resist bloodstream movement. Therefore, the mechanical properties of scaffold are a problem worthy of our attention. The results in Figure 2D, E and F showed that the tensile strength and elongation at break of the other SF/fibrin scaffolds were significantly improved, but the Young's modulus was reduced, when compared to the pure fibrin scaffold. More specifically, the mechanical strength of four SF/fibrin scaffolds increased significantly with the increase of SF content.

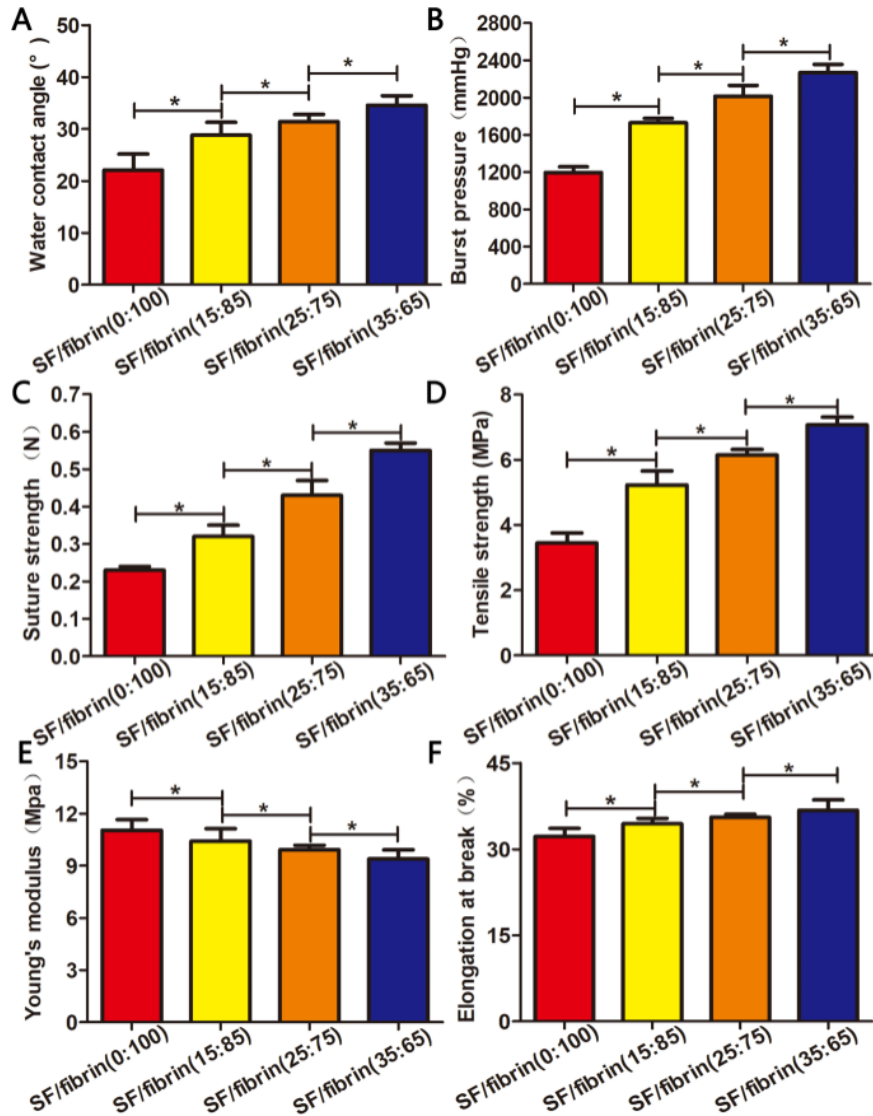


Fig. 2. Analysis of hydrophilicity and mechanical properties of four SF/fibrin vascular scaffolds. Water contact angel of the four electrospun scaffolds (A). The burst pressure (B), suture strength (C), tensile strength (D), Young's modulus (E) and elongation at break (F) of the four SF/fibrin scaffolds (n=3). indicated P < 0.05.

3.3 Hemocompatibility of SF/fibrin vascular scaffolds

The schematic diagram of platelet adhesion and red blood cell incubation on scaffold materials were showed in Figure 3A. Compared with the control group, hemolysis rarely occurred on the four vascular scaffold materials. Furthermore, the hemolysis value of four different SF/fibrin scaffolds were lower than 2%, and less than the American Society for Testing and Materials standard value of 5% (Figure3B). To study the behavior of platelets on different vascular scaffolds, we analyzed their morphology by SEM. From the SEM images, we found that a small amount of sporadic platelets adhered to the surface of different vascular materials, and then no significant phenomenon of aggregation and deformation (Figure3C and D). This indicated that the vascular scaffold had excellent anticoagulant function. Interestingly, there was no significant deformation of erythrocyte morphology on fibrin and SF/fibrin electrospun membranes, which further indicated that these vascular materials had good hydrophilic properties (Figure3E and F).

Plasma recalcification time (PRT) is an experimental indicator of endogenous coagulation system defects. The PRT value of SF/fibrin (0:100), SF/fibrin (15:85), SF/fibrin (25:75) and SF/fibrin (35:65) electrospun vascular scaffolds were 175s,178s,184s and186s, respectively. Meanwhile,there were no statistical difference between their groups, and then the PRT value decreased slightly with the increase of SF content (Figure3G). Moreover, the results showed that TT values in four different SF/fibrin electrospun scaffolds were all in normal safety values (15–18s) (Figure 3H). Surprisingly, with the increased of SF content in SF/fibrin scaffolds, the value of APTT did not transform significantly (Figure 3I).

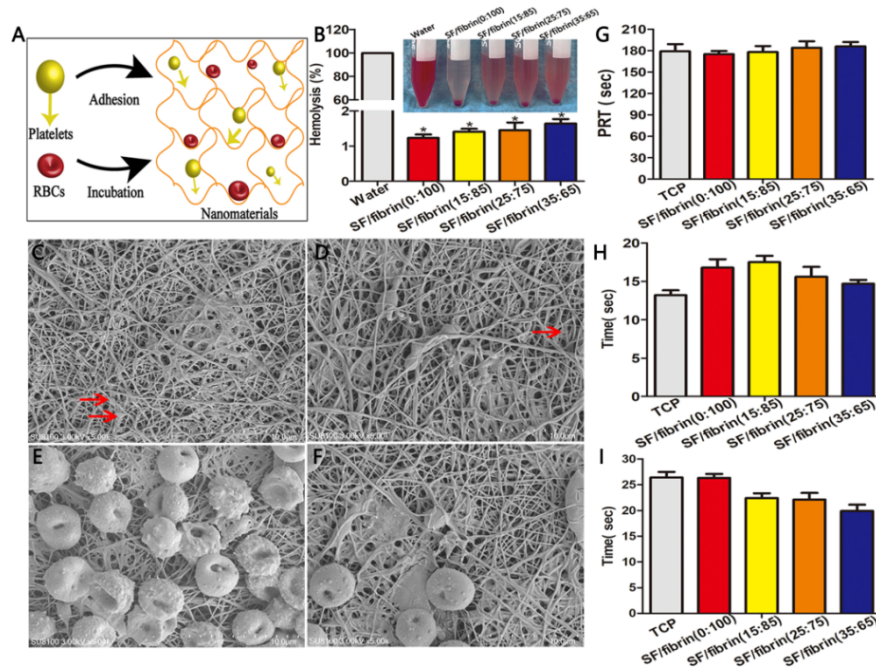


Fig. 3. Schematic diagram of platelet adhesion and red blood cell incubation on vascular scaffolds(A). Hemolysis rate of four different scaffolds material(B). Images of platelet adhesion in SF/fibrin(C) and fibrin(D) samples under SEM. The red arrows referred to platelets adhered by the SEM. The SEM photos of the red blood cells incubated with fibrin(E) and SF/fibrin(F) vascular scaffold for 3 hours. The Plasma recalcification time (G), TT (H) and APTT (I) were evaluated (n=3). indicated P < 0.05.

3.4 The biodegradability and cell growth with scaffold extract

To explore the stability of different SF/fibrin scaffolds, we investigated its degradability in vitro. The degradation of scaffold materials includes water degradation and enzyme degradation which were shown in

Fig.4A. As the degradation time prolonged, the mass of different SF/fibrin scaffolds decreased. Remarkably, we found that the mass loss rate of the four scaffolds in PBS hydrolysis were much lower than that in lipase (Figure 4B and C). We also observed that the degradation of composite scaffolds added SF component were slower. The degradation rate of SF/fibrin (0:100) electrospun scaffolds was higher than that of the other three composite scaffolds in PBS degradation (Figure 4B). Moreover, the mass loss rate at lipase degradation of SF/fibrin (15:85), SF/fibrin (25:75) and SF/fibrin (35:65) scaffolds were all lower than those of SF/fibrin (0:100) scaffolds after 4 weeks (Figure 4C).

After 2, 4 and 6 days of culture different scaffold extracts and RADMSCs, we found that the cells grew in a typical spindle shape or fish school shape under the microscope. Concurrently, the morphology of these cells had not changed significantly. In addition, the number of cells in different sample groups were not statistically significant. The images of three different groups showed that the corresponding cell amount increased gradually with the prolongation of cultured time (Figure 4D).

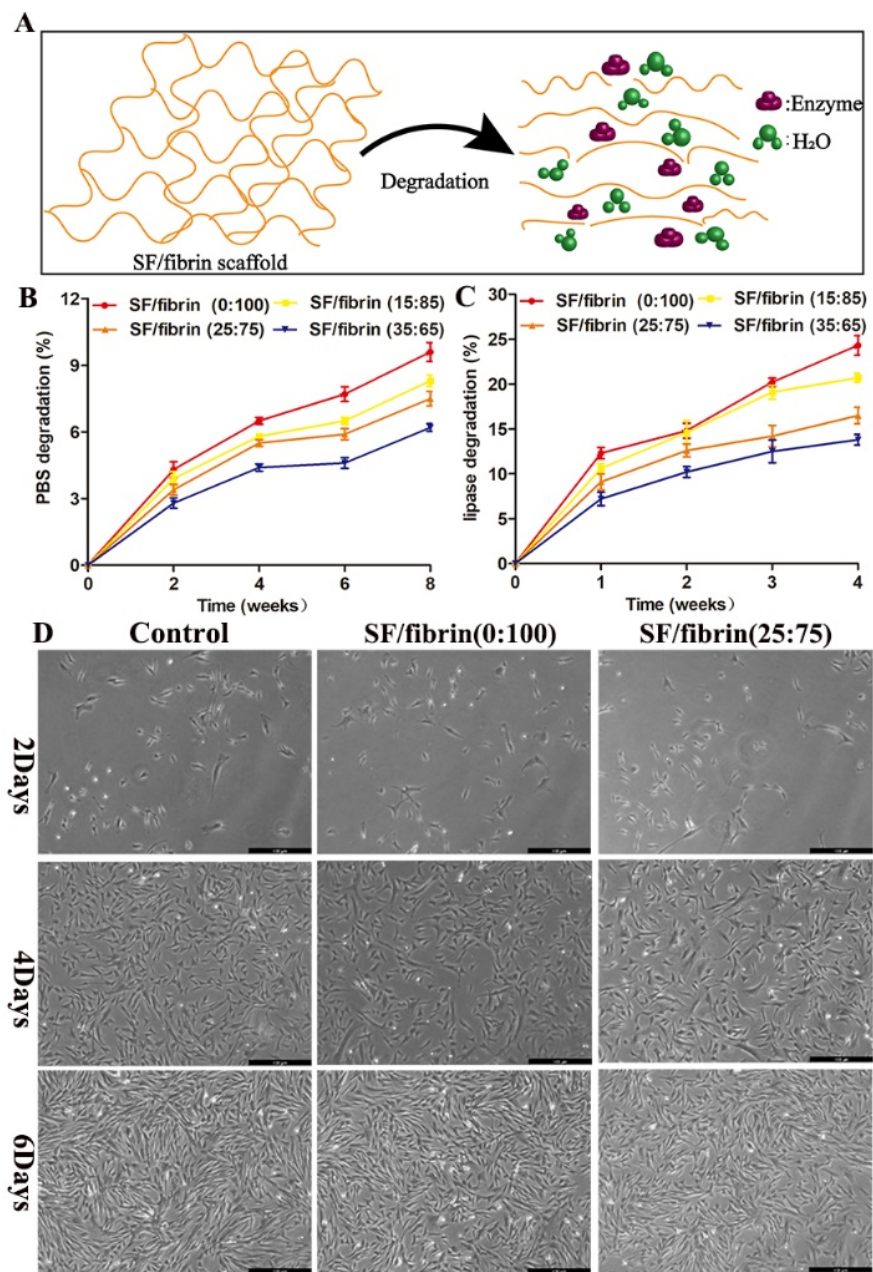


Fig. 4. Schematic diagram of the degradation characterizations of SF/fibrin scaffold in vitro(A). The PBS degradation (B) and lipase degradation(C) of SF/fibrin electrospun materials with different mass ratios were analyzed. The images of RADMSCs were cultured on different scaffold extract at 2, 4 and 6 days respectively (D). Scale bar: 100 μ m.

3.5 Cell proliferation characteristics of SF/fibrin scaffold

To analyze the scaffold materials affected the cell activity, we used RADMSCs as model cells and cocultured them with four SF/fibrin electrospun membranes (Figure5A). The proliferation behavior of the cells on different samples was assessed by a CCK-8 kit assay. The results indicated that the number of cells on

different scaffold materials increased significantly with time. Concurrently, there were no significant differences between all four groups after 1 day. Besides, we were surprised to observe that there was significant statistical difference between SF/fibrin (35:65) group and other groups at 3 days of coculture. Interestingly, the cell proliferation of the four scaffold groups were statistically significant at 7 days (Figure5B). After 1,3 and 5 days of coculture, the viability of the cells on different vascular materials was evaluated by a living cell staining test (Figure5C). Live cells are transformed into fluorescent calcein by non-fluorescent Calcein AM in this kit, which is the green fluorescence. We successfully cultured the cells on different scaffold materials for 1, 3, and 5 days, respectively. Regardless of the day, the images showed that these cells on the random vascular scaffolds had no obvious orientation. The results clearly indicated that the number of living cells on SF/fibrin (15:85) and SF/fibrin (25:75) scaffolds was more than that on SF/fibrin (0:100) at different time points. However, the number of living cells on the SF/fibrin (35:65) scaffolds was much lower than that on other groups.

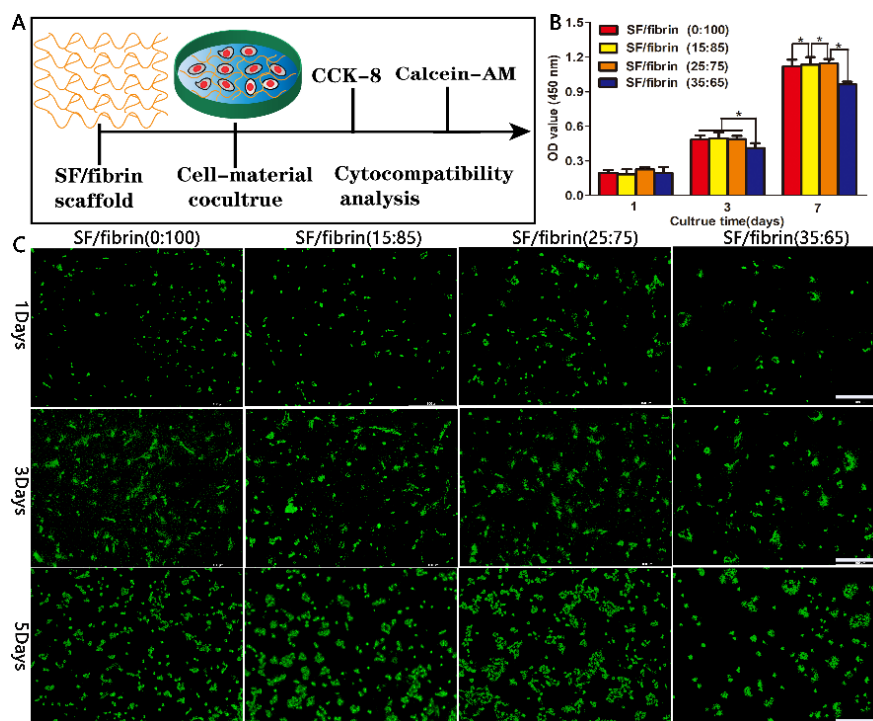


Fig. 5. Proliferation behavior of RADMSCs on four SF/fibrin electrospun scaffolds. The schematic diagram of the cytocompatibility test of scaffold materials in vitro(A). The optical density 450 values of the CCK-8 experiment was evaluated on 1, 3 and 7 days(B)(n=3). Live (green) staining of the cells cultured on four SF/fibrin blended scaffolds after different time points(C). The scale bar was 100 μ m. indicated P < 0.05.

3.6 Analysis of cytoskeletal by fluorescence staining

After 4 days and 7 days of culturing, the cells adhesion and growth on the surface of four different vascular scaffolds were evaluated by actin(red) and DAPI (blue) staining assay. The cytoskeleton stained by actin antibody spread homogeneously along the directional direction of the MSCs on all different SF/fibrin electrospun membranes (Figure6A). Compared with 4 days of cultured, the cell proliferation on the electrospun SF/fibrin scaffolds surface were extremely prosperous at 7 days. Shockingly, the number of positive cells on both SF/fibrin (0:100), SF/fibrin (15:85) and SF/fibrin (25:75) scaffold was significantly higher than the SF/fibrin (35:65) scaffold. At the same time, we found that the expression of actin on the surface of all four scaffold groups also increased with the prolong of culture time. To further verify this conclusion, these values were analyzed by Image J software. The statistical analysis confirmed that the number of cells on SF/fibrin

(25:75) electrospun materials was far more than that on the other groups after the 4 days and 7 days, and then they were statistically significant (Figure 6B and 6C). Furthermore, the number of cells on SF/fibrin (35:65) group was statistically different from other groups at the predetermined time point.

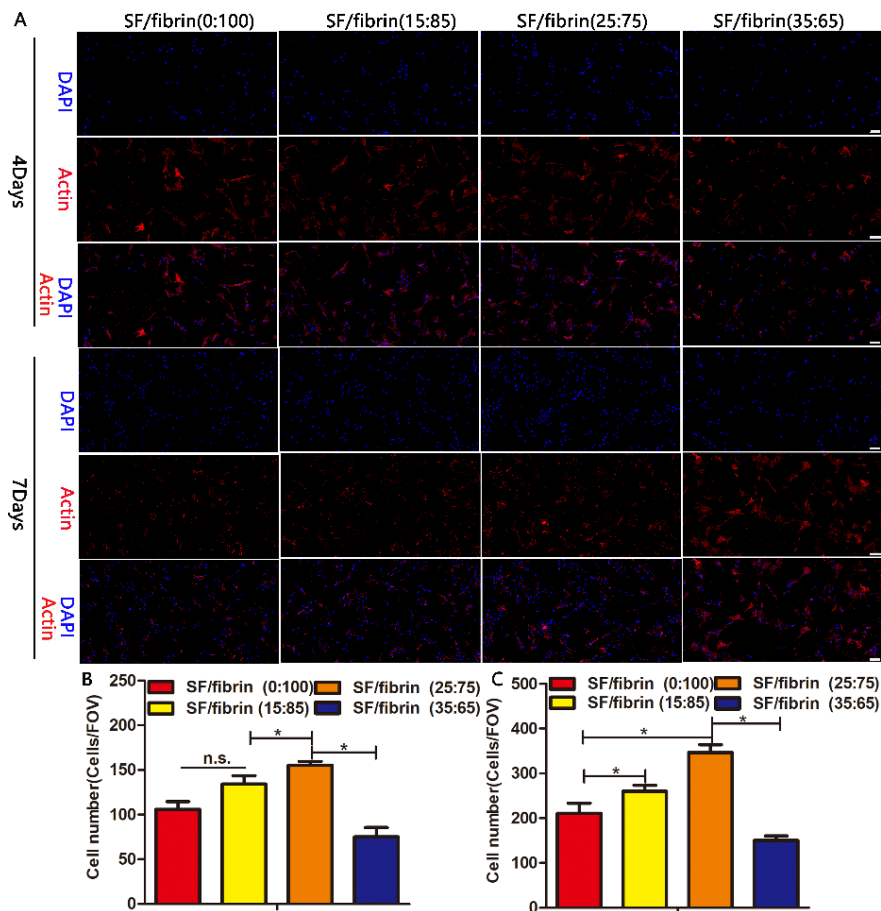


Fig. 6. The adhesion of RADMSCs on different SF/fibrin electrospun membranes. The cytoskeleton (red) and DAPI (blue) staining images of the cells cultured on the scaffold material after 4 and 7 days, respectively(A). Scale bar=100 μ m. Quantitative evaluation of cell number in the four groups after 4 days (B) and 7 days (C)of cultured (n=3). indicated $P < 0.05$. n.s. represented no statistical significance.

3.7 Subcutaneous implantation of the vascular scaffold and degradation in vivo

Different electrospun materials were further implanted into animals to observe their degradation behavior in vivo (Fig. 7A). During the in vivo animal experiment, these SD rats showed no obvious signs of surgical incision infection and no other adverse disease complications. Meanwhile, the sham surgery control group was established. Furthermore, we analyzed the morphological changes of electrospun scaffolds to investigate the in vivo degradation of different vascular materials after implantation. Two weeks after implantation, different scaffold materials had been completely wrapped by surrounding tissues. Moreover, we found that changed obviously in the appearance of different electrospun membranes. After these scaffolds were completely removed from the implantation site, we observed that the size of SF/fibrin (25:75) scaffold material was smaller than that of SF, which implied some degree of degradation (Fig. 7B). Meanwhile, we analyzed that the degradation rate of SF vascular scaffolds was lower than that of SF/fibrin (25:75) scaffolds, but the degradation rate of pure fibrin scaffolds was higher than their group. Four weeks after implantation, the

degradation rate of SF, SF/fibrin (25:75) and fibrin scaffolds were 14.34%, 21.20% and 25.76%, respectively (Fig. 7C).

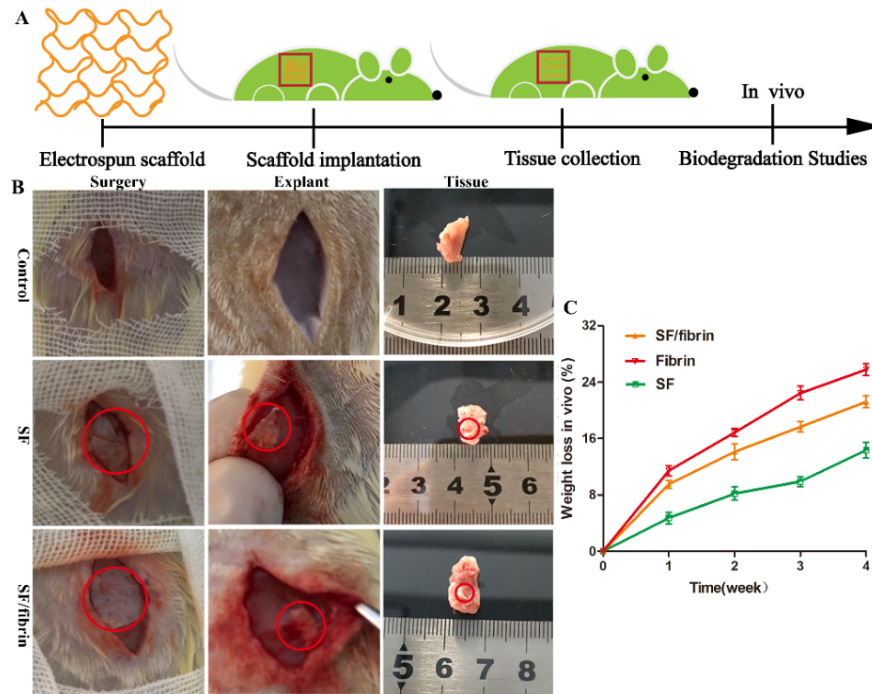


Fig.7. The schematic image of vascular scaffold degradation in vivo(A). Gross observation of different vascular scaffolds after subcutaneous implantation for 2 weeks(B). Red circles indicated electrospun scaffold materials. The weight loss changes of three different scaffold in vivo degradation(C).

3.8 Investigation of host histology in vivo

The results confirmed that compared with the control group, the SF scaffold and SF/fibrin (25:75) scaffold more obviously induced the host tissue inflammatory cell infiltration after 1 week of implantation. At 2 weeks post-implantation, the degree of inflammatory reaction in all groups decreased significantly compared with that before implantation. At the same time, the inflammatory reaction in SF/fibrin (25:75) group was milder than that in SF group (Fig. 8A). To evaluate the content of collagen deposition in blue, we used Masson's trichrome staining. From Masson staining images, we found that there was remarkable collagen deposition in different groups, and then the SF scaffold induced more sparser fibrous capsules than the SF/fibrin (25:75) scaffold at 1 and 2 weeks. These results confirmed that the SF/fibrin (25:75) scaffold developed abundant and well-organized structure of collagen. But SF exhibited some the fibrous electrospun scaffold structure and a small amount of newly collagen formation. Moreover, quantitative analysis results confirmed that the thickness of collagen layer in SF/fibrin (25:75) vascular scaffold was significantly higher than that of SF, but lower than that of the control group (Fig. 8B). The CD68 antibody markers were used to analyze the inflammatory response of three different samples. After 1 week, the immunohistochemistry images of CD68 showed that the SF scaffolds induced immune response was significantly stronger than that in SF/fibrin (25:75) scaffold. Interestingly, we were surprised to observe that the expression level of CD68 in all groups showed a decreasing trend with the prolongation of implantation time. What's more, the quantitative calculation results showed that the expression of CD68 positive cells in SF group was significantly higher than that in the other two groups. Furthermore, there was no significant difference in the number of CD68 cells between SF/fibrin and the control group at 2 weeks (Fig. 8C).

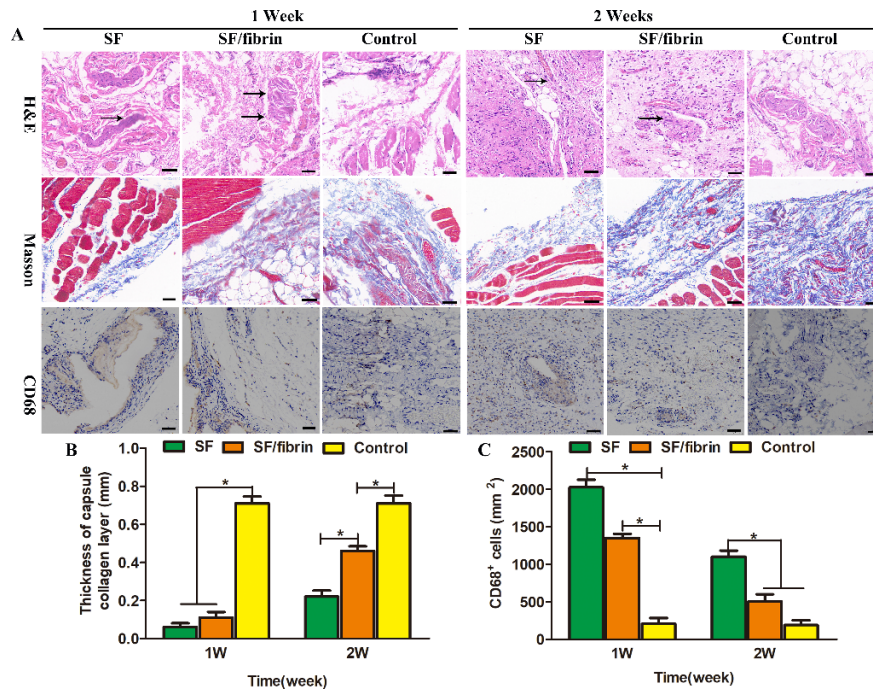


Fig.8. Histological images of SF group, SF/fibrin (25:75) and control group after subcutaneous implantation for 1 week or 2 weeks (A). The scale bar of H&E staining, Masson staining and CD68 staining images indicated 50 μ m, respectively. The black arrowed marked the scaffold. The quantitative evaluation of thickness of capsule collagen layer(B) and CD68 positive cells(C) in different groups(n=3). *P < 0.05 in (B) and (C).

4. Discussion

Many researchers have already confirmed that the ideal preparation factors for small-diameter tissue engineering vascular scaffold should be stable mechanical strength, biodegradability, excellent biocompatibility, minimal immune rejection and easy operation.¹⁹ Meanwhile, qualified vascular scaffolds should also have the function of regeneration and vascular reconstruction in vivo.²⁰ Moreover, some outstanding scientists have successfully used SF and fibrin as raw materials to construct artificial vascular scaffolds, which have been widely applied to small-caliber tissue engineering blood vessels.²¹⁻²² In our article, we mainly used electrospinning technology to fabricate SF/fibrin composite materials with different mass ratios, and then systematically analyzed the mechanical properties, hemocompatibility, degradability, cytocompatibility, and biocompatibility of the vascular scaffolds. The results showed that the SF/fibrin fiber scaffolds were uniformly distributed, with a smooth surface and suitable porosity (Fig.1C1-C4). Above all, the results showed that the fiber diameter of the electrospun vascular materials decreased gradually with the increase of SF content in SF/fibrin scaffolds. This is mainly due to the density of SF/fibrin spinning solution increased after the addition of SF, thereby enhancing the conductivity, and then spraying relatively smaller fiber diameter (Fig.1D1-D4).

Generally speaking, the hydrophilicity of biomaterial surface seriously affects the biocompatibility of the vascular scaffold. Researchers have demonstrated that the surface of suitable hydrophilic substances was promoted for cell growth, proliferation, and adhesion.²³⁻²⁴ From Figure 2A, we were surprised to that the water contact angle of the vascular scaffold also increased significantly with the increase of SF content in SF/fibrin scaffold. These results may be explained by the increased of β -sheet structure in SF molecules, which prevented water molecules from infiltrating into it, and then led to the decrease of hydrophilicity. Therefore, the hydrophilic property of the composite scaffold was greatly enhanced by the addition of fibrin material with good hydrophilicity. Furthermore, the mechanical properties are an important reference index for tissue engineering vascular scaffolds. Artificial vascular scaffolds with mechanical properties similar to

native vessels can not only bear the blood flow force, but also maintain the normal shape of the vascular lumen.²⁵The burst strength reflects that the artificial scaffold resistance to blood pressure *in vivo*, which is an important evaluation factor. In this study, the burst pressure value of SF/fibrin (15:85), SF/fibrin (25:75) and SF/fibrin (35:65) electrospun scaffolds were higher than those of the human native blood vessels(1500mmHg) and similar to the saphenous veins(1680~2273 mmHg).²⁶⁻²⁷This results further confirmed that SF/fibrin vascular scaffolds met the requirements of tissue engineering blood vessels. The suture strength is the maximum suture tension between the scaffold material and the vascular anastomosis. From Figure 2C, the suture strength values of SF/fibrin(25:75) and SF/fibrin(35:65) vascular scaffolds were 0.43 N and 0.55 N, respectively, which indicated that they were closed to the requirements of artificial blood vessels (0.5 N).²⁸Additionally, the results showed that the tensile strength value and the elongation at break value of four SF/fibrin vascular scaffolds increased obviously with increase SF content. All these results confirmed that the addition of SF could significantly enhance the mechanical properties of SF/fibrin electrospun scaffolds. Nevertheless, the elastic modulus values of different SF/fibrin vascular scaffolds showed that the addition of SF could improve their elastic deformation ability. More importantly, related studies have demonstrated that the β -sheet content of SF was directly proportional to co-relation of mechanical properties.²⁹Hence, the results of this mechanical strength may be closely related to the format of SF material and the degree of crystallization and its β -sheet formation.

Various physical and chemical reasons cause the rupture and dissolution of red blood cells, and then the release of hemoglobin, which is called hemolysis.³⁰The results from Figure 3B showed that all SF/fibrin electrospun scaffolds were not more than 2%, which confirmed that the vascular scaffold had reliable safety in clinical application. Platelet adhesion refers to the physiological function that platelets can adhere to collagen tissue and the surface of foreign bodies, and then it is a major reason for vascular materials to promote thrombotic transduction.³¹This consequences that may be due to the successful mixing of fibrin material with superior hydrophilicity and SF material with rich negative charge, thereby greatly reducing the number of platelet adhesion of SF/fibrin vascular scaffolds. Furthermore, the red blood cells on different nanomaterials exhibited good morphology. We analyzed from the results that the hydrophilic SF/fibrin scaffolds had excellent compatibility with red blood cells.³²The PRT was evaluated to express the time at which coagulation occurred in the electrospun scaffold after calcium ion addition.³³We found that there was no significant statistical difference in PRT values of four different SF/fibrin electrospun scaffolds. These results demonstrated that the blood compatibility of the scaffold had no impact with the increased of SF content. Recently, APTT and TT experiments are widely used to analyze the antithrombogenicity function of biomaterials *in vitro*. Our results further showed that the anticoagulation effect of SF/fibrin composite scaffold had no significant influence after changing SF content.

During the remodeling process of artificial blood vessels, a balance should be provided between the degradation rate of ideal biomaterials and the regeneration of tissue cells *in vivo*.³⁴The results from Figure 4B showed that the degradation rate of all SF/fibrin scaffolds in PBS increased as the fibrin was decreased. Specifically, the mass loss of SF/fibrin (0:100) scaffold was higher than that of other groups after 8 weeks of degradation. Li et al.³⁵ had successfully confirmed that fibrin gel could be used as an ideal biodegradable scaffold, and the material adhered to native tissues after its degradation, which was beneficial to cell migration, attachment and proliferation. In the meantime, we found that the trend of results in enzymatic degradation was comparable to that in PBS (Figure 4C). This may be due to the corresponding biochemical reaction that occurs when the enzyme enters the internal active site of the scaffold, resulting in the destruction of the molecular structure of the composite scaffold.³⁶This phenomenon indicated that fibrin had excellent degradation performance. Another, good biological characteristics is another important parameter for the development of an ideal electrospun vascular scaffold. Therefore, we designed related experiments *in vitro* to analyze the biocompatibility of SF/fibrin electrospun scaffolds. From the results, we observed that these cells in the SF/fibrin group exhibited superior cell migration, attachment, and viability compared with those in the control group after 2, 4, and 6 days of cultured (Figure 4D). This may be the result of the collaborative role of SF and fibrin in the cellular response of MSCs.

At the present time, numerous scientific researchers have prepared vascular materials by electrospinning

to mimic the structure and functionality of the extracellular matrix, which could significantly improve the growth and proliferation behavior of cells.³⁷ For example, Karkan et al.³⁸ analyzed the compatibility between PU/PCL nanofibers with different ratios and HUVECS, and then the results confirmed that the cells on vascular materials exhibited good proliferation behavior. In the CCK-8 experimental consequences, we analyzed that the cell counts on all four SF/fibrin vascular scaffolds with different mass ratios increased with prolonged of time (Figure 5B). After 3 and 7 days of co-culture, the cell proliferation on SF/fibrin (0:100), SF/fibrin (15:85) and SF/fibrin (25:75) scaffolds was significantly better than that on SF/fibrin (35:65). This results fully confirmed that the SF/fibrin (25:75) electrospun scaffolds could effectively improve the cell proliferation behavior on the scaffold material, and then the vascular scaffold had particularly few toxic reactions. To better verify this phenomenon, we evaluated it by living cell fluorescence experiment. By fluorescence staining microscope, we observed that these cells on four SF/fibrin scaffolds groups showed good growth and adhesion ability at the specific time point. Besides, compared to the other three groups, the number of live cells on SF/fibrin (35:65) vascular scaffolds was the lowest (Figure 5C). A series of results further indicated that SF/fibrin (25:75) vascular scaffold exhibited excellent cytocompatibility which could be considered as one of the ideal tissues engineering vascular scaffold.

To further evaluate the activity of cells on different vascular scaffolds at specific time points, we carried out a series of related immunofluorescence experiments. Many reports have shown that the chemical and composition changes in pure SF vascular scaffold prepared by electrospinning could effectively improve its cell viability. Furthermore, as medical suture material of SF had displayed good biocompatibility to many types of cells and could promote the growth of vascular cells.³⁹ In our research work, we were surprised to observe that the number of cells in the SF/fibrin (25:75) group was higher than that in the SF/fibrin (15:85) and SF/fibrin (35:75) group. Meanwhile, the results in Figure 6 showed that the SF/fibrin (15:85) group was slightly more than the SF/fibrin (0:100) group. This may be due to the high surface to volume ratio and nanofibrous biomimetic architecture of the vascular scaffolds prepared by electrospinning technology, which is more conducive to the attachment and growth of the cells on the scaffold materials. We also analyzed the proliferation morphology of different electrospun scaffolds under a fluorescence microscope. All our results indicated that SF/fibrin composite vascular materials exhibited superior biocompatibility.

For the application of vascular scaffold, the in vivo degradation rate should match the tissue regeneration rate, which is a crucial factor.⁴⁰ The degradation of biomaterials is mainly influenced by bioactive substances such as enzymes, microenvironment, the structure and morphological, and then macrophages. Wang et al.⁴¹ prepared regenerated silk fibroin three-dimensional porous scaffolds to evaluate their degradation behavior in rats at 8 weeks and 1 year, respectively. We concluded that the degradation in vivo of the scaffold was influenced by multiple factors such as its preparation method, structural composition and immune response, which further showed that the in vivo degradation of scaffold was predictability and controllability. Our research results indicated that the degradation rate of SF/fibrin vascular scaffolds in vivo was higher than that of SF scaffolds. At the same time, the size of different electrospun samples decreased with the increased of implantation time, and they adhered to the surrounding tissues (Figure 7B). We analyzed that SF with a content of silk II structure may effectively reduce the degradation rate of the biomaterial. Additionally, compared to fibrin scaffold with higher degradation rate and SF scaffold with lower degradation rate, SF/fibrin can maintain a reasonable degradation rate in vivo, which greatly improves tissue regeneration and remodeling.

Implantation of electrospun scaffold materials into SD rats can commonly lead to inflammatory body reaction, and then adhere to the host tissue for fibrous encapsulation.⁴² The surrounding explants were removed for histological evaluation after 1 and 2 weeks. We confirmed from the results that the surrounding tissues of SF and SF/fibrin scaffolds demonstrated significant inflammatory cell response. Meanwhile, the expression of macrophages in different samples was further evaluated by CD68 staining. The number of CD68 cells in SF/fibrin scaffold was less than that in SF scaffold, and then the expression level of CD68 in all samples changed with the implantation time (Figure 8). We confirmed from the results that the SF/fibrin scaffold could be effectively improved the cellular infiltration and phenotype change of macrophages. Collagen deposition, as a key factor of vascular regeneration is the main component of constructing extracellular

matrix. The results indicated that the SF/fibrin scaffolds had thicker collagen than the SF scaffolds at different times, but still slightly lower than in control group. We analyzed that the SF/fibrin vascular scaffold had good tissue regeneration ability and could be used as an ideal artificial blood vessel scaffold.

5. Conclusion

In this paper, SF/fibrin vascular scaffold was successfully fabricated by electrospinning equipment. It was found that the fiber diameter of pure fibrin scaffold was significantly larger than that of other mass ratio SF/fibrin scaffolds. We analyzed from the results that the mechanical performances of SF/fibrin scaffolds obviously increased with the increase of SF content, but significantly affected the surface hydrophilicity and degradation rate of vascular scaffolds. Nevertheless, the SF content of SF/fibrin scaffold was 35%, and the cell compatibility was obviously impaired. Therefore, SF/fibrin (25:75) electrospun scaffold indicated balanced mechanical strength, excellent hemocompatibility, biodegradability and cytocompatibility. Importantly, a series of experiments in vivo showed that the degradation rate of SF/fibrin scaffold was higher than that of SF scaffold. Meanwhile, the expression of collagen in SF/fibrin (25:75) vascular scaffolds was higher than that in pure SF scaffolds, but their macrophage content was relatively low. This study confirmed that SF/fibrin scaffold was considered as a candidate material for small diameter tissue engineering vascular scaffolds.

Disclosure statement

The authors declared that they have no conflicts of interest to this work. We declare that we have no commercial or affiliate interests representing any conflict of interest with respect to the submitted work.

Acknowledgements

Our work was financially supported by the Science and Technology Plan of Guangzhou city Project (202102020485), Doctoral workstation foundation of Puning city TCM hospital (BSGZZ2021001), Scientific research project of Guangdong Provincial Bureau of Traditional Chinese Medicine (20221474), Science and technology plan project of science and technology bureau of Jieyang (ylxm037), Guangzhou science and technology plan city-school joint project (2023A03J0266), Science and Technology Plan of Guangzhou city Project (202102020108), Guangdong Medical Science and Technology Research Fund Project (A2023336).

References

1. Semachew A. Global Burden of Cardiovascular Diseases and Risk Factors, 1990–2019. *The American Journal of Cardiology*.2020;76 (25):2982-3021.
2. Mathers CD, Loncar D. Projections of Global Mortality and Burden of Disease from 2002 to 2030. *PLOS Medicine*. 2006;3(11).
3. Townsend N, Wilson L, Bhatnagar P, et al. Cardiovascular disease in Europe: epidemiological update 2016 (vol 37, pg 3232, 2017). *European Heart Journal: The Journal of the European Society of Cardiology*. 2019;2 (40):189-189.
4. Hassen H Y, Bowyer M, Gibson L, et al. Level of cardiovascular disease knowledge, risk perception and intention towards healthy lifestyle and socioeconomic disparities among adults in vulnerable communities of Belgium and England. *BMC Public Health*. 2022;22 (1):1-9.
5. Bolger A P, Coats AJS, Gatzoulis MA. Congenital heart disease: the original heart failure syndrome. *European Heart Journal*. 2003;10 (10):970-976.
6. Cao Y L, Liu W, Zhang W J, et al. Recent progress in tissue engineering. *Journal of Shanghai Jiaotong University (Medical Science)* .2012;32 (9):1241-1250.
7. Xue L, Greisler H P. Biomaterials in the development and future of vascular grafts. *Journal of vascular surgery*.2003;37 (2):472-480.
8. Tong W, Chen H, Mo XM. A new vascular tissue engineering material: Electrospun small-diameter nanofibrous scaffolds. *Chinese Journal of Tissue Engineering Research*. 2013.

9. Kim SH, Kwon JH, Kim YH, et al. Fabrication of a new tubular fibrous PLCL scaffold for vascular tissue engineering. 2006;17(12):1359-1374
10. Arenas JE, Ahn Hill, TK Young, et al. Dual seeded polycaprolactone (PCL)/collagen electrospun vascular scaffold for engineering small diameter blood vessel and clinical translation. Journal of the American College of Surgeons. 2012;215(3):S139-S140.
11. El Maachi I, Kyriakou S, Rütten S, et al. Silk Fibroin as Adjuvant in the Fabrication of Mechanically Stable Fibrin Biocomposites. Polymers (Basel). 2022;14(11):2251.
12. Ansari AI, Sheikh N A. Biocompatible Scaffold Based on Silk Fibroin for Tissue Engineering Applications. 2022.
13. Alireza N, Jamal AS, Roza VG, et al. A review of fibrin and fibrin composites for bone tissue engineering. International Journal of Nanomedicine. 2017;12:4937-4961.
14. Zhao L, Li X, Yang L, et al. Evaluation of remodeling and regeneration of electrospun PCL/fibrin vascular grafts in vivo. Materials Science and Engineering C. 2020;118 (12):111441.
15. Yang L, Li X, Wang D, et al. Improved mechanical properties by modifying fibrin scaffold with PCL and its biocompatibility evaluation. Journal of Biomaterials Science. 2020;5 (31):
16. Yang L, Li X, Wu Y, et al. Preparation of PU/Fibrin Vascular Scaffold with Good Biomechanical Properties and Evaluation of Its Performance in vitro and in vivo. International journal of nanomedicine. 2020;15:8697-8715.
17. Promita, Bhattacharjee, Julia, et al. Potential for combined delivery of riboflavin and all-trans retinoic acid, from silk fibroin for corneal bioengineering. Materials Science & Engineering C. 2019; 105 (Dec):.1-14.
18. Salehi A, Nourbakhsh MS, Rafienia M, et al. Corneal stromal regeneration by hybrid oriented poly (ϵ -caprolactone)/lyophilized silk fibroin electrospun scaffold. International Journal of Biological Macromolecules. 2020;161:377-378.
19. Rotmans J I, Campbell J H. Tissue engineering for small-diameter vascular grafts. Biointegration of Medical Implant Materials.2010:116-146.
20. Wu P, Wang L, Li W, et al. Construction of vascular graft with circumferentially oriented microchannels for improving artery regeneration. Biomaterials. 2020;242:119922.
21. Brougham C, Jockenhoevel S, Flanagan T, et al. A Collagen-Glycosaminoglycan-Fibrin Scaffold For Heart Valve Tissue Engineering Applications, 6th Biennial Heart Valve Biology & Tissue Engineering Meeting 10th-12th September .2014;9.
22. Couet F, Rajan N, Vesentini S, et al. Design of a Collagen/Silk Mechano-Compatible Composite Scaffold for the Vascular Tissue Engineering: Focus on Compliance. Key Engineering Materials.2007; 334-335 (Pt2):1169-1172.
23. Karkan S F, Rahbarghazi R, Davaran S, et al. Electrospun polyurethane/poly (epsilon-caprolactone) nanofibers promoted the attachment and growth of human endothelial cells in static and dynamic culture conditions. Microvascular research. 2021;133:104073.
24. Jin D, Hu J, Xia D, et al. Evaluation of a simple off-the-shelf bi-layered vascular scaffold based on poly(L-lactide-co- ϵ -caprolactone)/silk fibroin in vitro and in vivo. International Journal of Nanomedicine .2019;1(14):4261-4276.
25. Pan, XN, Li YX, Jiang L H. Tissue-engineered vascular scaffold materials. Chinese Journal of Tissue Engineering Research. 2016;34
26. Nafiseh J, Davod M K, Abdolreza S, et al. Small-diameter vascular graft using co-electrospun of composite PCL/PU nanofibers. Biomedical Materials.2018;13(5):1748-6041.

27. Konig G, Mcallister TN, et al. Mechanical properties of completely autologous human tissue engineered blood vessels compared to human saphenous vein and mammary artery. *Biomaterials*. 2009; 30 (8):1542-1550.
28. Asvar Z, Mirzaei E, Azarpira N, et al. Evaluation of electrospinning parameters on the tensile strength and suture retention strength of polycaprolactone nanofibrous scaffolds through surface response methodology. *Journal of the Mechanical Behavior of Biomedical Materials*. 2017;75:369-378.
29. Behera, Sibaram, Chen, et al. Guangqiang, et al. Exploration of the tight structural-mechanical relationship in mulberry and non-mulberry silkworm silks. *Journal of Materials Chemistry B Materials for Biology & Medicine*.2016.
30. Wang D, Wang X, Li X, et al. Biologically responsive, long-term release nanocoating on an electrospun scaffold for vascular endothelialization and anticoagulation. *Materials science & engineering*. 2020;107 (Feb.): 1-11.
31. Motlagh D, Yang J, Lui, et al. Hemocompatibility evaluation of poly(glycerol-sebacate) in vitro for vascular tissue engineering. *Biomaterials*.2006;27 (24):4315-4324.
32. Saha K, Moyano DF, Rotello VM. Protein coronas suppress the hemolytic activity of hydrophilic and hydrophobic nanoparticles. *Mater Horiz*. 2013;1 (1):102-105.
33. Espadastorre C, Meyerhoff M E. Thrombogenic Properties of Untreated and Poly(ethylene oxide)Modified Polymeric Matrixes Useful for Preparing Intraarterial Ion Selective Electrodes. *Analytical Chemistry*. 1995;67 (18):3108-3114.
34. A L L, A S J P, B M D L, et al. In vitro degradation of porous poly(l-lactic acid) foams - ScienceDirect. *Biomaterials*.2000;21 (15):1595-1605.
35. Li Y, Meng H, Yuan L, et al. Fibrin Gel as an Injectable Biodegradable Scaffold and Cell Carrier for Tissue Engineering. *The scientific world journal*. 2015;2015:685690.
36. Ulery BD, Nair LS, Laurencin CT. Biomedical applications of biodegradable polymers. *Journal of Polymer Science Part B Polymer Physics*.2011;49 (12):832-864.
37. Xu S, Yan X, Zhao Y, et al. In vitro biocompatibility of electrospun silk fibroin mats with Schwann cells. *Journal of Applied Polymer ence*. 2010;119 (6):3490-3494.
38. Karkan SF, Rahbarghazi R, Davaran S, et al. Electrospun polyurethane/poly (-caprolactone) nanofibers promoted the attachment and growth of human endothelial cells in static and dynamic culture conditions. *Microvascular Research*. 2020;(133) :104073.
39. Alessandrino A, Chiarini A, Armato A, et al. Three-Layered Silk Fibroin Tubular Scaffold for the Repair and Regeneration of Small Caliber Blood Vessels: From Design to in vivo Pilot Tests. *Frontiers in Bioengineering and Biotechnology* .2019;7:356.
40. W ZA, Ping LB, Gang SA, et al. Appropriately adapted properties of hot-extruded Zn-0.5Cu-xFe alloys aimed for biodegradable guided bone regeneration membrane application. *Bioactive Materials*. 2021;6 (4):975-989.
41. Wang Y, Rudym DD, Walsh A, et al. In vivo degradation of three-dimensional silk fibroin scaffolds. *Biomaterials*. 2008;29 (24-25):3415-3428.
42. Heymann F, Trotha KTV, Preisinger C, et al. Polypropylene mesh implantation for hernia repair causes myeloid cell-driven persistent inflammation. *JCI Insight*. 2019;4 (2): e123862.

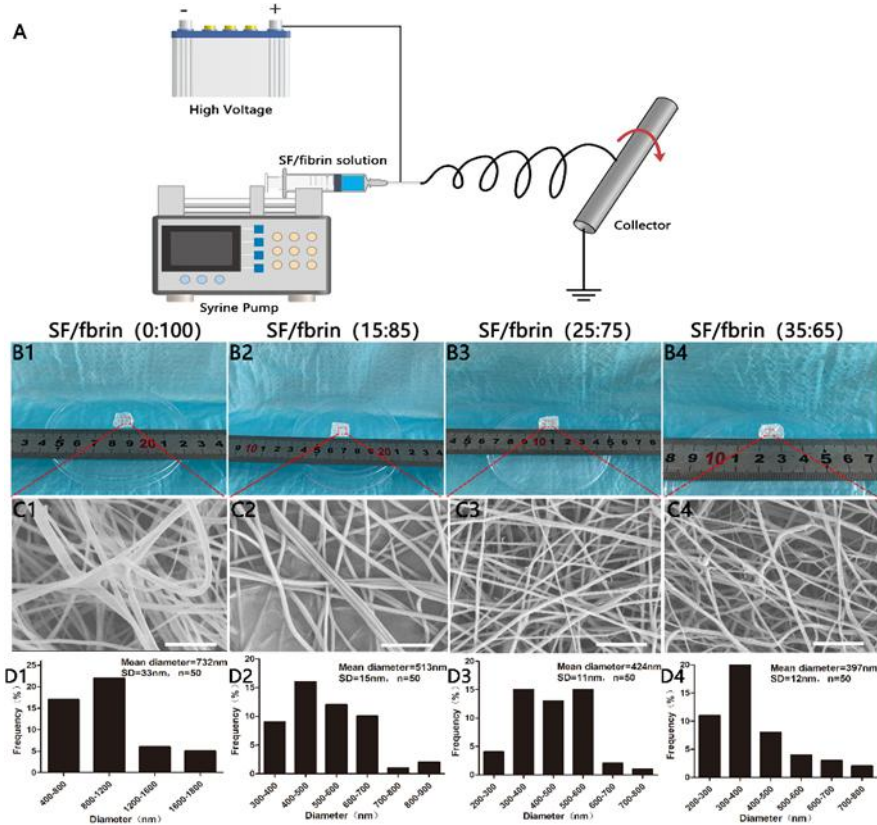


Fig. 1. Fabrication and characterization of the electrospun vascular scaffold. Schematic diagram of electrospun SF/fibrin hybrid scaffolds(A). The macroscopic appearance of SF/fibrin scaffolds with different mass ratios(B1-B4). SEM images of four electrospun scaffolds(C1-C4). Scale bars:10 μ m. Fiber diameter distribution of different SF/fibrin scaffolds by ImageJ software (D1-D4) (n=3).

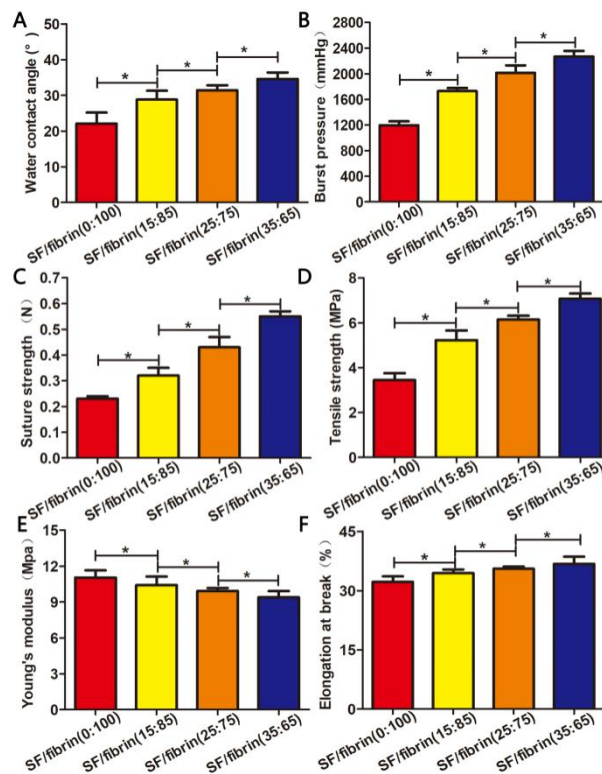


Fig. 2. Analysis of hydrophilicity and mechanical properties of four SF/fibrin vascular scaffolds. Water contact

angel of the four electrospun scaffolds (A). The burst pressure (B), suture strength (C), tensile strength (D), Young's modulus (E) and elongation at break (F) of the four SF/fibrin scaffolds (n=3). ★ indicated P < 0.05.

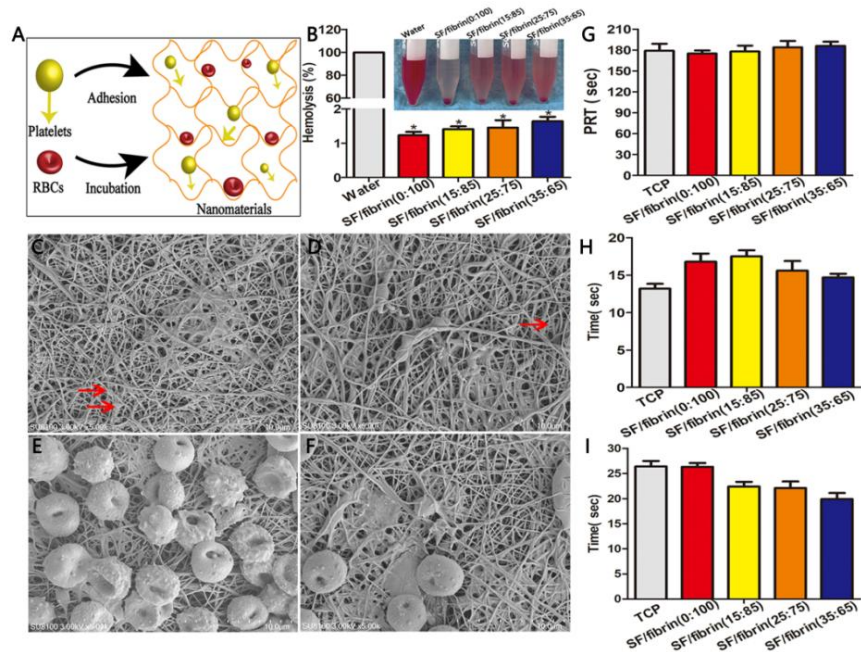


Fig. 3. Schematic diagram of platelet adhesion and red blood cell incubation on vascular scaffolds(A). Hemolysis rate of four different scaffolds material(B). Images of platelet adhesion in SF/fibrin(C) and fibrin(D) samples under SEM. The red arrows referred to platelets adhered by the SEM. The SEM photos of the red blood cells incubated with fibrin(E) and SF/fibrin(F) vascular scaffold for 3 hours. The Plasma recalcification time (G), TT (H) and APTT (I) were evaluated (n=3). ★ indicated P < 0.05.

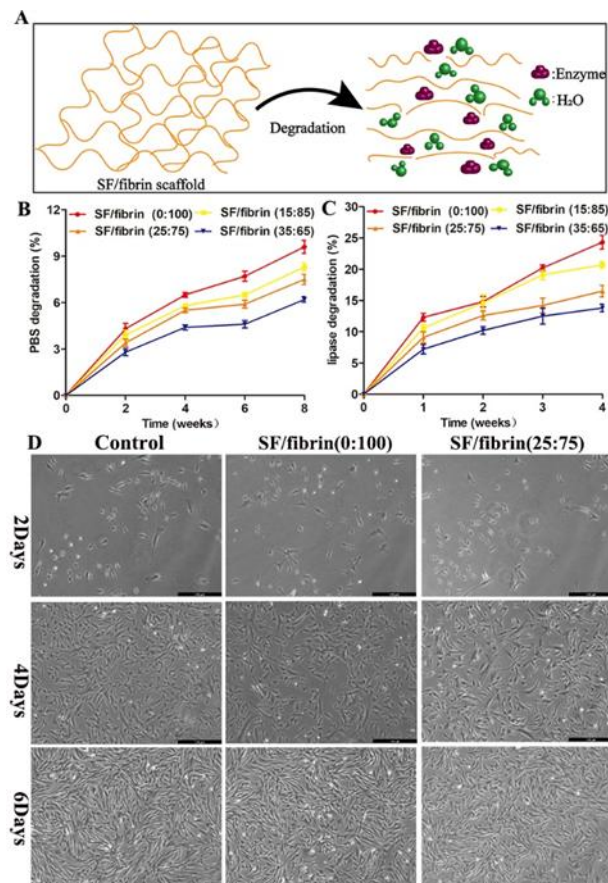


Fig. 4. Schematic diagram of the degradation characterizations of SF/fibrin scaffold in vitro(A). The PBS degradation (B) and lipase degradation(C) of SF/fibrin electrospun materials with different mass ratios were analyzed. The images of RADMSCs were cultured on different scaffold extract at 2, 4 and 6 days respectively (D). Scale bar: 100 μ m.

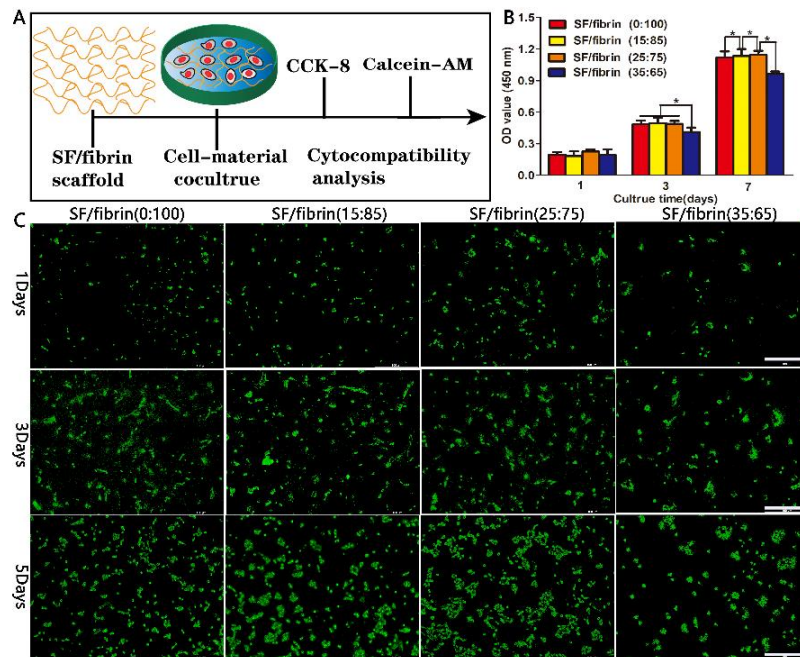


Fig. 5. Proliferation behavior of RADMSCs on four SF/fibrin electrospun scaffolds. The schematic diagram of the cytocompatibility test of scaffold materials in vitro(A). The optical density 450 values of the CCK-8 experiment was evaluated on 1, 3 and 7 days(B)(n=3). Live (green) staining of the cells cultured on four SF/fibrin blended scaffolds after different time points(C). The scale bar was 100 μ m. ★indicated P < 0.05.

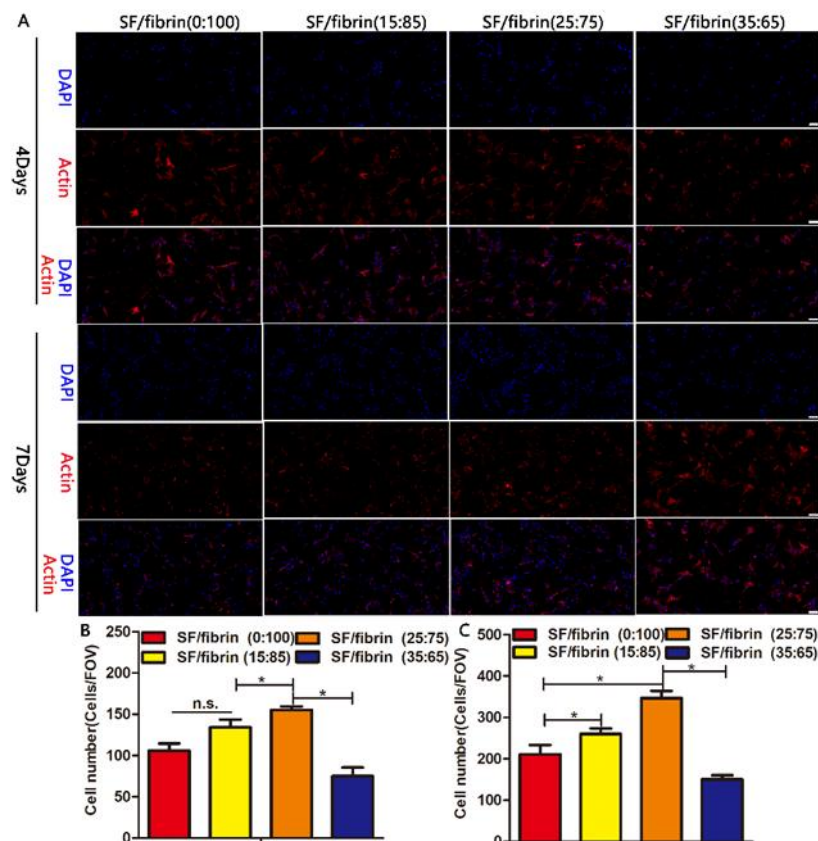


Fig. 6. The adhesion of RADMSCs on different SF/fibrin electrospun membranes. The cytoskeleton (red) and DAPI (blue) staining images of the cells cultured on the scaffold material after 4 and 7 days, respectively(A). Scale bar=100 μ m. Quantitative evaluation of cell number in the four groups after 4 days (B) and 7 days (C)of cultured (n=3). ★ indicated P<0.05. n.s. represented no statistical significance.

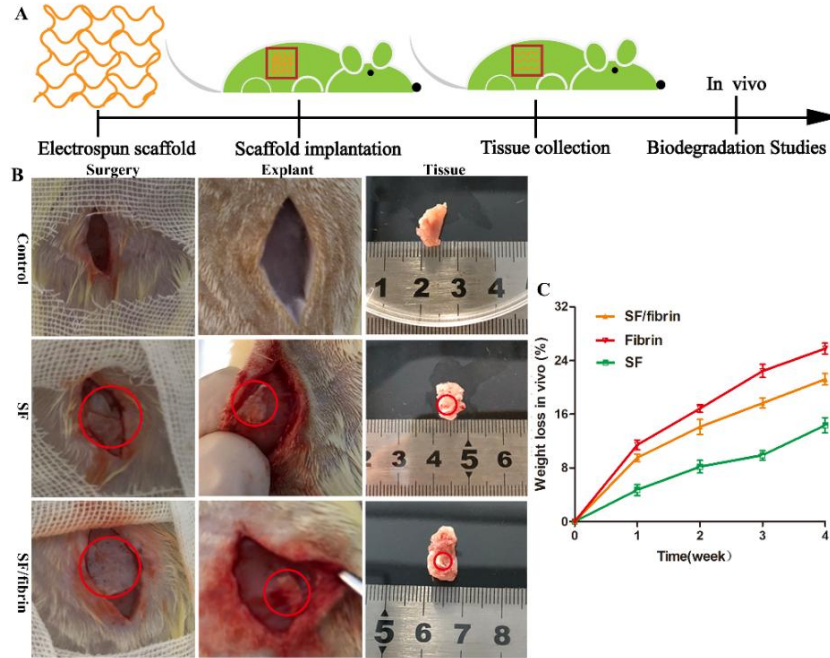


Fig.7. The schematic image of vascular scaffold degradation in vivo(A). Gross observation of different vascular scaffolds after subcutaneous implantation for 2 weeks(B). Red circles indicated electrospun scaffold materials. The weight loss changes of three different scaffold in vivo degradation(C).

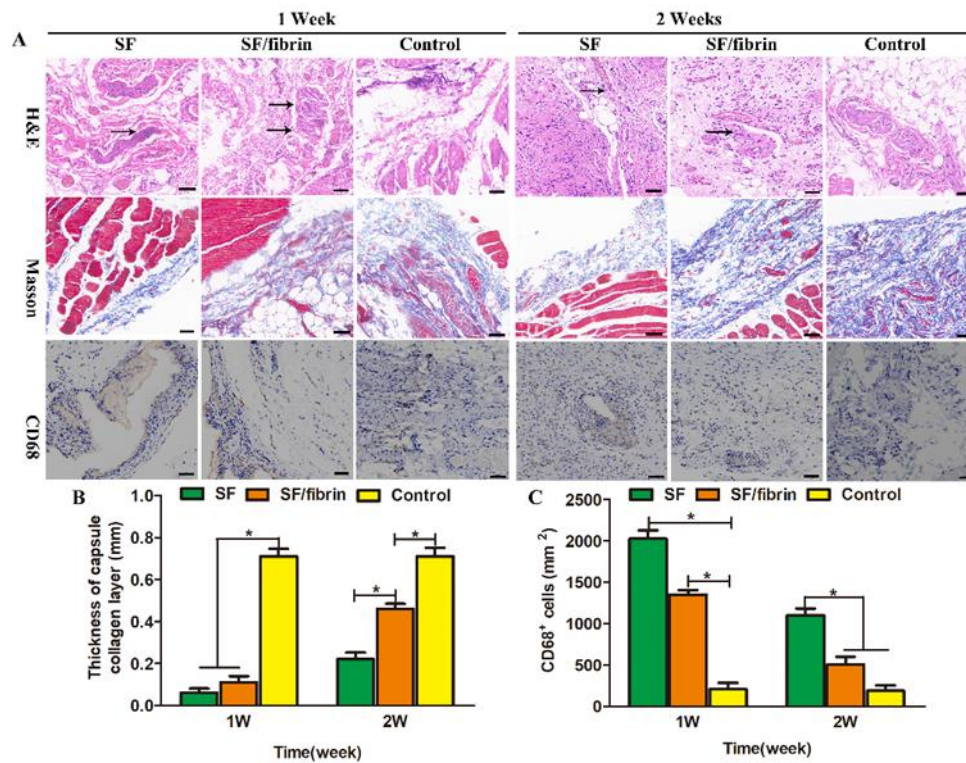


Fig.8. Histological images of SF group, SF/fibrin (25:75) and control group after subcutaneous implantation for 1

week or 2 weeks (A). The scale bar of H&E staining, Masson staining and CD68 staining images indicated 50 μ m, respectively. The black arrowed marked the scaffold. The quantitative evaluation of thickness of capsule collagen layer(B) and CD68 positive cells(C) in different groups(n=3). *P < 0.05 in (B) and (C).